WIDEBAND CHANNEL TRACKING FOR MILLIMETER WAVE MASSIVE MIMO SYSTEMS WITH HYBRID BEAMFORMING RECEPTION

George C. Alexandropoulos[1]*, Evangelos Vlachos*[2]*, and John Thompson*[2]

[1]Department of Informatics and Telecommunications, National and Kapodistrian University of Athens, Panepistimiopolis Ilissia, 15784 Athens, Greece
[2]Institute for Digital Communications, University of Edinburgh, EH9 3JL Edinburgh, UK
emails: alexandg@di.uoa.gr, {e.vlachos, j.s.thompson}@ed.ac.uk

ABSTRACT

Millimeter Wave (mmWave) massive Multiple Input Multiple Output (MIMO) channel tracking is a challenging task with Hybrid analog and digital BeamForming (HBF) reception architectures. The wireless channel can only be spatially sampled with directive analog beams, which results in lengthy training periods when beam codebooks are large. In this paper, we capitalize on a recently proposed HBF architecture enabling mmWave massive MIMO channel estimation with short beam training overhead, and present a matrix-completion-based channel tracking technique for time correlated HBF receivers. The considered channel tracking problem is formulated as a constrained multi-objective optimization problem incorporating the low rank and group-sparse properties of the mmWave channel as well as a popular model for its time correlation. We present an efficient algorithm for this estimation problem that is based on the alternating direction method of multipliers. Comparisons of the proposed approach over representative state-of-the-art techniques showcase the relation between the channel time correlation coefficient and the amount of beam training needed for acceptable channel estimation performance.

Index Terms— Channel tracking, millimeter wave communications, massive multiple-input multiple-output (MIMO), alternating direction method of multipliers (ADMM).

1. INTRODUCTION

The millimeter Wave (mmWave) frequency band is one of the key enablers for the highly demanding data rate requirements of fifth Generation (5G), and beyond, wireless networks [1] offering large communication bandwidths. The Hybrid analog and digital BeamForming (HBF) transceiver architectures [2] have been recently considered in the specifications of the 5G New Radio (NR) [3] and IEEE 802.11ay technologies targeting tens of Gbit/s data rate mmWave communications. This architecture is intended for cost and operationally feasible wideband mmWave massive Multiple Input Multiple Output (MIMO) systems realizing directive communication capable to confront the high propagation losses in the involved frequencies. However, the hardware limitations with large antenna HBF receivers and the short coherence time of wideband mmWave massive MIMO channels render the reliable and time efficient channel tracking a very challenging task.

The explicit estimation of mmWave massive MIMO Channel State Information (CSI) from HBF receivers with predefined sets of analog beams [4, 5, 6, 7] has been mainly treated as a compressive sensing problem [8], where the Orthogonal Matching Pursuit (OMP) algorithm [9] was usually adopted to recover the sparse channel gain vector. However, the performance of the compressive-sensing-based CSI estimation techniques is usually limited by the codebook design, since beam dictionaries suffer from power leakage due to the discretization of the Angle of Arrival (AoA) and Angle of Departure (AoD). In [10, 11, 12], the sparsity and low rank properties of mmWave MIMO channels were jointly exploited for efficient CSI estimation. The matrix-completion-based approach of [12] was very recently extended to wideband channels in [13] using a modified HBF architecture for training measurements collection. Wideband mmWave MIMO channels with frequency selectivity were also considered in [7], where a CSI estimation technique exploiting channel's sparsity in both time and frequency domains was presented.

In this paper, we present a novel low overhead mmWave massive MIMO channel tracking algorithm that is based on the HBF receiver architecture proposed in [13]. We adopt a time correlation model for the channel gain evolution and formulate a novel constrained multi-objective optimization problem for CSI tracking that is efficiently solved via the Alternating Direction Method of Multipliers (ADMM).

2. SYSTEM AND CHANNEL MODELS

2.1. System Model

We assume single-carrier communication in a frame-by-frame basis operating over mmWave multipath fading MIMO channels, where the channel remains constant during each frame but changes in a correlated manner from one frame

to the following ones. Every frame consists of T training symbols dedicated for CSI estimation, whereas the rest of the frame is used for data communication. Obviously, a large T facilitates improved CSI estimation, but leaves less frame length for actual data communication. To estimate the wideband mmWave MIMO channel between a N_{T}-antenna Transmitter (TX) and an intended HBF Receiver (RX) with N_{R} antenna elements attached to $M_{\mathrm{R}} \ll N_{\mathrm{R}}$ Radio Frequency (RF) chains, the TX utilizes the $N_{\mathrm{T}} \times 1$ training symbols' vector $\mathbf{s}[t]$ for each slot t with $t = 1, 2, \ldots, T$. It can be shown [13] that the $N_{\mathrm{R}} \times T$ complex-valued received training signal at the intended HBF reception node is expressed as

$$\mathbf{Y} \triangleq \sum_{k=1}^{N_{\mathrm{T}}} \tilde{\mathbf{H}}_k \mathbf{\Psi}_k + \mathbf{N}, \tag{1}$$

where $\tilde{\mathbf{H}}_k \triangleq [\mathbf{h}_k(1)\, \mathbf{h}_k(2) \cdots \mathbf{h}_k(L)] \in \mathbb{C}^{N_{\mathrm{R}} \times L}$ with $\mathbf{h}_k(\ell)$ being the k-th column of the ℓ-th (with $\ell = 1, 2, \ldots, L$) delay tap of the MIMO channel matrix $\mathbf{H}(\ell) \in \mathbb{C}^{N_{\mathrm{R}} \times N_{\mathrm{T}}}$. Each (ℓ, t)-th element of each $L \times T$ Toeplitz matrix $\mathbf{\Psi}_k$ is given by $[\mathbf{\Psi}_k]_{\ell,t} \triangleq s_k[t - L - \ell + 1]$, where the symbol $s_k[t]$ represents the k-th element of the N_{T}-element complex-valued training vector $\mathbf{s}[t]$ at time slot t. Finally, $\mathbf{N} \in \mathbb{C}^{N_{\mathrm{R}} \times T}$ in (1) is the Additive White Gaussian Noise (AWGN) matrix with independent and identically distributed entries each having zero mean and variance σ_n^2.

2.2. Channel Model

We consider the temporally correlated mmWave channel model of [14, 15], where the gain, AoA, and AoD of the channel at the n-th frame are obtained from the respective ones of the channel at the $(n-1)$-th frame. Specifically, we consider that the n-th frame channel matrix for the ℓ-th delay tap can be expressed as

$$\mathbf{H}_n(\ell) = \mathbf{A}_{\mathrm{R}}(\boldsymbol{\theta}_n) \mathrm{diag}\{\mathbf{a}_n(\ell)\} \mathbf{A}_{\mathrm{T}}^H(\boldsymbol{\phi}_n), \tag{2}$$

where matrices $\mathbf{A}_{\mathrm{T}}(\boldsymbol{\phi}_n) \in \mathbb{C}^{N_{\mathrm{T}} \times N_p}$ and $\mathbf{A}_{\mathrm{R}}(\boldsymbol{\theta}) \in \mathbb{C}^{N_{\mathrm{R}} \times N_p}$ are defined as

$$\mathbf{A}_{\mathrm{T}}(\boldsymbol{\phi}_n) \triangleq \left[\mathbf{A}_{\mathrm{T}}([\boldsymbol{\phi}_n]_1)\ \mathbf{A}_{\mathrm{T}}([\boldsymbol{\phi}_n]_2) \cdots \mathbf{A}_{\mathrm{T}}\left([\boldsymbol{\phi}_n]_{N_p}\right)\right], \tag{3a}$$

$$\mathbf{A}_{\mathrm{R}}(\boldsymbol{\theta}_n) \triangleq \left[\mathbf{A}_{\mathrm{R}}([\boldsymbol{\theta}_n]_1)\ \mathbf{A}_{\mathrm{R}}([\boldsymbol{\theta}_n]_2) \cdots \mathbf{A}_{\mathrm{R}}\left([\boldsymbol{\theta}_n]_{N_p}\right)\right]. \tag{3b}$$

In the latter expressions, variable $[\boldsymbol{\phi}_n]_p \in [0, 2\pi]$ with $p = 1, 2, \ldots, N_p$ denotes the p-th path's AoD from TX at the n-th frame and variable $[\boldsymbol{\theta}_n]_p \in [0, 2\pi]$ represents the p-th path's AoA at RX at the n-th frame. In addition, $\mathbf{A}_{\mathrm{T}}([\boldsymbol{\phi}_n]_p) \in \mathbb{C}^{N_{\mathrm{T}} \times 1}$ and $\mathbf{A}_{\mathrm{R}}([\boldsymbol{\theta}_n]_p) \in \mathbb{C}^{N_{\mathrm{R}} \times 1}$ are the array response vectors at TX and RX, respectively (for uniform linear antenna arrays, these vectors are given by [4, eq. (5)]). In (2), $\mathbf{a}_n(\ell) \in \mathbb{C}^{N_p \times 1}$ includes the path channel gains at the n-th frame and $\mathrm{diag}\{\mathbf{a}_n(\ell)\} \in \mathbb{C}^{N_p \times N_p}$ is a diagonal matrix with $\mathbf{a}_n$'s elements on its main diagonal.

We assume that the channel gains vector at each ℓ-th delay tap of each n-th frame follow the first-order Auto Regressive (AR) model:

$$\mathbf{a}_n(\ell) = \rho \mathbf{a}_{n-1}(\ell) + \bar{\rho} \boldsymbol{\beta}, \tag{4}$$

where $\rho \in [0, 1]$ denotes the time correlation coefficient and $\bar{\rho} \triangleq \sqrt{1 - \rho^2}$. The parameter ρ is given by the Jakes' model $\rho = J_0(2\pi f_{\mathrm{D}} T_{\mathrm{coh}})$ with $J_0(\cdot)$ denoting the zeroth order Bessel function of the first kind, f_{D} being the maximum Doppler frequency, and T_{coh} is the channel coherence time. Vector $\boldsymbol{\beta} \in \mathbb{C}^{N_p \times 1}$ has entries drawn from the Zero Mean Complex Gaussian Distribution (ZMCGD) that are independent from those in $\mathbf{a}_{n-1}(\ell)$. It is also assumed that the AoAs and AoDs of the L propagation paths do not change between different frames, i.e., $\forall n$ holds $\boldsymbol{\phi}_n = \boldsymbol{\phi}$ and $\boldsymbol{\theta}_n = \boldsymbol{\theta}$.

The latter assumptions can be alternatively incorporated into the beamspace representation of the mmWave MIMO channel [16]. To this end, $\mathbf{H}_n(\ell)$ in (2) is re-expressed as

$$\mathbf{H}_n(\ell) = \mathbf{D}_{\mathrm{R}} \mathbf{Z}_n(\ell) \mathbf{D}_{\mathrm{T}}^H, \tag{5}$$

where $\mathbf{D}_{\mathrm{R}} \in \mathbb{C}^{N_{\mathrm{R}} \times N_{\mathrm{R}}}$ and $\mathbf{D}_{\mathrm{T}} \in \mathbb{C}^{N_{\mathrm{T}} \times N_{\mathrm{T}}}$ are unitary matrices based on the discrete Fourier transform, and $\mathbf{Z}_n(\ell) \in \mathbb{C}^{N_{\mathrm{R}} \times N_{\mathrm{T}}}$ includes the virtual channel gains of $\mathbf{H}_n(\ell)$. Motivated by the low rank property of $\mathbf{H}_n(\ell)$, we further assume that $\mathbf{Z}_n(\ell)\ \forall \ell$ contains only few virtual channel gains with high amplitude, i.e., it is a sparse matrix. Its sparsity level depends on the angular discretization in the beamspace representation of (5). Using the notations $\bar{\mathbf{H}}_n \triangleq [\mathbf{H}_n(1)\, \mathbf{H}_n(2) \cdots \mathbf{H}_n(L)] \in^{N_{\mathrm{R}} \times L N_{\mathrm{T}}}$ and $\bar{\mathbf{Z}}_n \triangleq [\mathbf{Z}_n(1)\, \mathbf{Z}_n(2) \cdots \mathbf{Z}_n(L)] \in^{N_{\mathrm{R}} \times L N_{\mathrm{T}}}$, (5) can be re-expressed as $\bar{\mathbf{H}}_n = \mathbf{D}_{\mathrm{R}} \bar{\mathbf{Z}}_n (\mathbf{I}_L \otimes \mathbf{D}_{\mathrm{T}}^H)$ with $\mathbf{I}_L$ being the $L \times L$ identity matrix and $\otimes$ represents the Kronecker product. Based on AR model in (4), we further express $\bar{\mathbf{Z}}_n$ as

$$\bar{\mathbf{Z}}_n = \rho \bar{\mathbf{Z}}_{n-1} + \bar{\rho}(\mathbf{\Omega}_S \circ \mathbf{U}_n), \tag{6}$$

where the real-valued $N_{\mathrm{R}} \times L N_{\mathrm{T}}$ matrix $\mathbf{\Omega}_S$ contains only zeros and ones, and the $N_{\mathrm{R}} \times L N_{\mathrm{T}}$ matrix $\mathbf{U}_n$ has elements drawn from ZMCGD with variance σ^2 resulting in small variations of the $\bar{\mathbf{Z}}_n$'s entries compared to the $\bar{\mathbf{Z}}_{n-1}$'s elements. The Hadamard product $\mathbf{\Omega}_S \circ \mathbf{U}_n$ constraints the update of the gains into specific areas in the two dimensional plane. The first-order AR time correlation model in (6) represents a slow time-varying channel, where the main propagation paths do not change in number neither in terms of their AoAs/AoDs.

2.3. Post-Processed Received Training Signals

By substituting (6) into (5) and then in (1), the received training signals for the n-th frame at the N_{R} antenna elements of the intended HBF receiver for the considered time correlation model can be expressed as

$$\begin{aligned} \mathbf{Y}_n &= \tilde{\mathbf{D}}_{\mathrm{R}}(\rho \bar{\mathbf{Z}}_{n-1} + \bar{\rho}(\mathbf{\Omega}_S \circ \mathbf{U}_n))(\mathbf{I}_L \otimes \mathbf{D}_{\mathrm{T}}^H)\bar{\mathbf{\Psi}} + \mathbf{N}_n \\ &= \rho \tilde{\mathbf{Y}}_{n-1} + \bar{\rho} \tilde{\mathbf{D}}_{\mathrm{R}} \tilde{\mathbf{U}}_n \mathbf{B}_n + \mathbf{N}_n, \end{aligned} \tag{7}$$

where $\bar{\mathbf{\Psi}} \triangleq [\mathbf{\Psi}^T(1)\,\mathbf{\Psi}^T(2)\cdots\mathbf{\Psi}^T(L)] \in \mathbb{C}^{LN_{\rm T}\times T}$ with $\mathbf{\Psi}(\ell) \in \mathbb{C}^{T\times N_{\rm T}}$ is obtained by concatenating each ℓ-th column from the $N_{\rm T}$ matrices $\mathbf{\Psi}_k$, $\tilde{\mathbf{Y}}_{n-1} \triangleq \tilde{\mathbf{D}}_{\rm R}\bar{\mathbf{Z}}_{n-1}\mathbf{B}_n$, $\tilde{\mathbf{U}}_n \triangleq \mathbf{\Omega}_S \circ \mathbf{U}_n$, $\mathbf{B}_n \triangleq (\mathbf{I}_L \otimes \mathbf{D}_{\rm T}^H)\bar{\mathbf{\Psi}}$, and $\mathbf{N}_n \in \mathbb{C}^{N_{\rm T}\times T}$ is the AWGN matrix at the n-th frame distributed as in (1). Eq. (7) uses the HBF reception architecture of [13], where $\tilde{\mathbf{D}}_{\rm R} \triangleq (\mathbf{W}_{\rm RF}^e)^H\mathbf{D}_{\rm R}$, where the complex-valued $N_{\rm R}\times N_{\rm R}$ matrix $\mathbf{W}_{\rm RF}^e$ denotes the analog receive combiner (i.e., in the RF domain) with unit magnitude and quantized phase elements [13, eq. (15)]. The latter signal is finally passed in the random spatial sampling unit, whose output is given by $\mathbf{R}_{\Omega,n} \triangleq \mathbf{\Omega}_n \circ \mathbf{Y}_n$, where the $N_{\rm R}\times T$ matrix $\mathbf{\Omega}_n$ is composed of $TM_{\rm R}$ ones and $T(N_{\rm R}-M_{\rm R})$ zeros. The positions of $\mathbf{\Omega}_n$'s unity elements in each of its rows are randomly chosen in a uniform fashion over the set $\{1,2,\ldots,N_{\rm R}\}$. Evidently, each column of $\mathbf{R}_{\Omega,n}$ will have only $M_{\rm R}$ non-zero rows out of its $N_{\rm R}$ in total, which will be fed to the $M_{\rm R}$ receive RF chains.

3. PROPOSED CHANNEL TRACKING ALGORITHM

We next present the proposed multi-objective problem formulation for wideband mmWave MIMO channel tracking and its designed ADMM-based optimum solution.

3.1. Problem formulation

We propose the following multi-objective mathematical formulation for the considered channel tracking problem:

$$\begin{aligned}\min_{\tilde{\mathbf{Y}}_n,\tilde{\mathbf{U}}_n}\ & \tau_Y\|\tilde{\mathbf{Y}}_n\|_* + \tau_Z\|\tilde{\mathbf{U}}_n\|_1 \\ & + \frac{1}{2}\|\tilde{\mathbf{Y}}_n - \rho\tilde{\mathbf{Y}}_{n-1} - \bar{\rho}\tilde{\mathbf{D}}_{\rm R}\tilde{\mathbf{U}}_n\mathbf{B}_n\|_F^2 \\ \text{s.t. }\ & \mathbf{R}_{\Omega,n} = \mathbf{\Omega}\circ\tilde{\mathbf{Y}}_n, \end{aligned} \tag{8}$$

where $\tau_R = 1/\|\mathbf{R}_{\Omega,n}\|_F^2$ and $\tau_Z = 1/\|\tilde{\mathbf{D}}_{\rm R}^\dagger\mathbf{R}_{\Omega,n}\mathbf{B}_n^\dagger\|_F^2$ are the weighting factors, and $(\cdot)^\dagger$ denotes the matrix pseudo-inverse operand. The term $\|\tilde{\mathbf{Y}}_n\|_*$ in the cost function of (8) enforces the low-rank property of the received training signals matrix $\tilde{\mathbf{Y}}_n$, where from (7) holds $\tilde{\mathbf{Y}}_n \triangleq \rho\tilde{\mathbf{Y}}_{n-1} + \bar{\rho}\tilde{\mathbf{D}}_{\rm R}\tilde{\mathbf{U}}_n\mathbf{B}_n$. Additionally, the term $\|\tilde{\mathbf{U}}_n\|_1$ promotes a sparse solution for $\tilde{\mathbf{U}}_n$. Finally, the last term in the cost function takes in to account the AWGN at the n-th frame, by minimizing the least-squares distance between the reconstructed noiseless data matrix $\tilde{\mathbf{Y}}_n$ and its updated version based on the considered time correlation channel model in (6).

3.2. Solution via ADMM

The optimization problem in (8) describes a highly coupled problem, thus, for it to be solved, the cost function has to be decomposed into multiple simpler subproblems. To do so, let us first introduce the following two auxiliary matrix variables $\mathbf{X}_n, \mathbf{C}_n \in \mathbb{C}^{N_{\rm R}\times T}$. Using the latter definitions, (8) can be equivalently expressed as

$$\begin{aligned}\min_{\tilde{\mathbf{Y}}_n,\tilde{\mathbf{U}}_n,\mathbf{X}_n,\mathbf{C}_n}\ & \tau_R\|\tilde{\mathbf{Y}}_n\|_* + \tau_Z\|\tilde{\mathbf{U}}_n\|_1 \\ & + \frac{1}{2}\|\mathbf{C}_n\|_F^2 + \frac{1}{2}\|\mathbf{\Omega}_n\circ\mathbf{X}_n - \mathbf{R}_{\Omega,n}\|_F^2 \\ \text{s.t. }\ & \tilde{\mathbf{Y}}_n = \mathbf{X}_n \text{ and } \mathbf{C}_n = \mathbf{X}_n - \rho\tilde{\mathbf{Y}}_{n-1} - \bar{\rho}\tilde{\mathbf{D}}_{\rm R}\tilde{\mathbf{U}}_n\mathbf{B}_n. \end{aligned} \tag{9}$$

The latter problem can be solved via alternating minimization over the four unknown variables, i.e., $\tilde{\mathbf{Y}}_n$, $\tilde{\mathbf{U}}_n$, $\mathbf{X}_n$, and $\mathbf{C}_n$. In this paper, we employ ADMM and we first obtain the

Algorithm 1 mmWave Massive MIMO Channel Tracking

Input: $\mathbf{R}_{\Omega,n}$, $\mathbf{\Omega}_n$, $\tilde{\mathbf{D}}_{\rm R}$, $\mathbf{B}_n$, τ_R, τ_Z, ρ, $\bar{\rho}$, $\tilde{\mathbf{U}}_{n-1}$, $\mathbf{X}_{n-1}$, $\mathbf{V}_{n-1}^{(1)}$, $\mathbf{V}_{n-1}^{(2)}$, $\mathbf{C}_{n-1}$, and $\mathbf{Y}_{n-1}$.

Output: $\tilde{\mathbf{U}}_n$, $\mathbf{X}_n$, $\mathbf{V}_n^{(1)}$, $\mathbf{V}_n^{(2)}$, $\mathbf{C}_n$, and $\mathbf{Y}_n$.

{**Minimization of $\mathcal{L}$ in** (10) **over** $\tilde{\mathbf{Y}}_n$}

1: $\tilde{\mathbf{Y}}_n = \text{SVT}_{\tau_Y/\gamma}(\mathbf{X}_{n-1} - \frac{1}{\gamma}\mathbf{V}_{n-1}^{(1)})$.

{**Minimization of $\mathcal{L}$ in** (10) **over** $\mathbf{X}_n$}

2: Solve the following linear system of equations:

$$\left(\sum_{j=1}^{N_{\rm R}}\text{diag}([\mathbf{\Omega}]_j)^T\otimes\mathbf{E}_{jj} + 2\gamma\mathbf{I}_{TN_{\rm R}}\right)\mathbf{x}_n = \text{vec}(\mathbf{V}_{n-1}^{(1)} + \gamma\mathbf{Y}_{n-1} + \mathbf{R}_{\Omega,n} + \mathbf{V}_{n-1}^{(2)} + \gamma\mathbf{C}_{n-1} + \gamma(\rho\tilde{\mathbf{Y}}_{n-1} + \bar{\rho}\tilde{\mathbf{D}}_{\rm R}\tilde{\mathbf{U}}_{n-1}\mathbf{B}_n))$$

with $\mathbf{E}_{jj}$ obtained from the $N_{\rm R}\times N_{\rm R}$ all-zero matrix after inserting a unity value at its (j,j)-th position.

3: Reshape vector $\mathbf{x}_n$ to matrix $\mathbf{X}_n$, i.e., $\mathbf{X}_n = \text{unvec}(\mathbf{x}_n)$.

{**Minimization of $\mathcal{L}$ in** (10) **over** $\tilde{\mathbf{U}}_n$}

4: $\boldsymbol{\xi} = (\mathbf{B}_n^T\otimes\tilde{\mathbf{D}}_{\rm R})^{-1}\text{vec}(\mathbf{X}_n - \mathbf{C}_{n-1} - \frac{1}{\gamma}\mathbf{V}_{n-1}^{(2)} - \gamma\tilde{\mathbf{Y}}_{n-1})$.

5: Apply the following soft-thresholding operator:

$$\begin{aligned}\tilde{\mathbf{u}}_n =& \text{sign}(\texttt{Re}(\boldsymbol{\xi}))\circ\max\left(|\texttt{Re}(\boldsymbol{\xi})| - \tau_Z/\gamma, 0\right) \\ & + \text{sign}(\texttt{Im}(\boldsymbol{\xi}))\circ\max\left(|\texttt{Im}(\boldsymbol{\xi})| - \tau_Z/\gamma, 0\right).\end{aligned}$$

6: Reshape vector $\tilde{\mathbf{u}}_n$ to matrix $\tilde{\mathbf{U}}_n$, i.e., $\tilde{\mathbf{U}}_n = \text{unvec}(\tilde{\mathbf{u}}_n)$.

{**Minimization of $\mathcal{L}$ in** (10) **over** $\mathbf{C}_n$}

7: $\mathbf{C}_n = \frac{\gamma}{1+\gamma}\left(\mathbf{X}_n - \rho\tilde{\mathbf{Y}}_{n-1} - \bar{\rho}\tilde{\mathbf{D}}_{\rm R}\tilde{\mathbf{Z}}_n\mathbf{B}_n - \frac{1}{\gamma}\mathbf{V}_{n-1}^{(2)}\right)$.

{**Update the dual variables**}

$$\begin{aligned}\mathbf{V}_n^{(1)} &= \mathbf{V}_{n-1}^{(1)} + \gamma\left(\mathbf{X}_n - \tilde{\mathbf{Y}}_n\right), \\ \mathbf{V}_n^{(2)} &= \mathbf{V}_{n-1}^{(2)} + \gamma\left(\mathbf{C}_n - \mathbf{X}_n + \rho\tilde{\mathbf{Y}}_{n-1} + \bar{\rho}\tilde{\mathbf{D}}_{\rm R}\tilde{\mathbf{U}}_n\mathbf{B}\right).\end{aligned}$$

Lagrangian function of the optimization problem (9) as:

$$\mathcal{L}(\tilde{\mathbf{Y}}_n, \tilde{\mathbf{U}}_n, \mathbf{X}_n, \mathbf{C}_n, \mathbf{V}_n^{(1)}, \mathbf{V}_n^{(2)}) \triangleq \tau_R \|\tilde{\mathbf{Y}}_n\|_* + \tau_Z \|\tilde{\mathbf{U}}_n\|_1 + \frac{1}{2}\|\mathbf{C}_n\|_F^2 + \frac{1}{2}\|\mathbf{\Omega} \circ \mathbf{X}_n - \mathbf{R}_{\Omega,n}\|_F^2 + \text{tr}((\mathbf{V}_n^{(1)})^H(\tilde{\mathbf{Y}}_n - \mathbf{X}_n)) + \frac{\gamma}{2}\|\tilde{\mathbf{Y}}_n - \mathbf{X}_n\|_F^2 + \text{tr}((\mathbf{V}_n^{(2)})^H(\mathbf{C}_n - \mathbf{X}_n + \rho\tilde{\mathbf{Y}}_{n-1} + \bar{\rho}\tilde{\mathbf{D}}_{\text{R}}\tilde{\mathbf{U}}_n)\mathbf{B}_n) + \frac{\gamma}{2}\|\mathbf{C}_n - \mathbf{X}_n + \rho\tilde{\mathbf{Y}}_{n-1} + \bar{\rho}\tilde{\mathbf{D}}_{\text{R}}\tilde{\mathbf{U}}_n\mathbf{B}_n)\|_F^2, \quad (10)$$

where $\mathbf{V}_n^{(1)} \in \mathbb{C}^{N_{\text{R}} \times T}$ and $\mathbf{V}_n^{(2)} \in \mathbb{C}^{N_{\text{R}} \times T}$ are dual variables (the Lagrange multipliers) adding the constraints of (9) to the cost function, and $\gamma \in (0, 1)$ denotes ADMM's stepsize. Due to space limitations, we omit the details for the latter steps in this paper, however, a similar procedure to [13] can be followed. The basic steps of the proposed solution are summarized in Algorithm 1. For the initialization at $n = 0$, we set: $\tilde{\mathbf{Y}}_0 = \tilde{\mathbf{U}}_0 = \mathbf{X}_0 = \mathbf{C}_0 = \mathbf{V}_0^{(1)} = \mathbf{V}_0^{(2)} = \mathbf{0}$, and in Step 1, the Singular Value Thresholding (SVT) operator [17] is used.

4. SIMULATION RESULTS AND DISCUSSION

In this section, we evaluate the performance of the proposed channel tracking technique taking place on a communication frame-by-frame basis. We consider an uplink scenario, where a TX user is equipped with an antenna array of size $N_{\text{T}} = 4$, while the HBF RX base station has $N_{\text{R}} = 32$ antennas. Although these values can be considered moderate in size for a massive MIMO scenario, upscaling the dimensions, while keeping the same ratio between the antenna array sizes of the TX and the RX is expected to give similar results. The number of the RF chains that connect the analog and digital HBF components at the base station side is $M_{\text{R}} = 16$. For the frequency selective mmWave MIMO channel, we have considered $L = 4$ delay taps and $N_p = 2$ propagation paths.

We first evaluate the Normalized Mean Squared Error (NMSE) performance of the estimated beamspace matrix $\hat{\bar{\mathbf{Z}}}_n$ at the n-th frame, defined as NMSE $\triangleq \|\bar{\mathbf{Z}}_n - \hat{\bar{\mathbf{Z}}}_n\|/\|\bar{\mathbf{Z}}_n\|$. We compare our ADMM-based technique to a state-of-the-art non-adaptive technique based on OMP [9], which exploits the common sparsity pattern between consecutive training slots within each frame. As a lower bound, we employ the OMP technique with a long training sequence $T = 80$, whose performance is determined by the AWGN level σ_n^2. We have also implemented the adaptive OMP-based approach "AdaOMP," which exploits only the estimated beamspace channel of the previous frame. For OMP and AdaOMP techniques, we have used the same T values as with our proposed one. In Fig. 1(a), we perform a sanity check on the convergence of the proposed technique with a short training sequence of $T = 20$, considering the case where the channel does not change over the frames, i.e., when $\rho = 1$. It is evident that the proposed technique converges to the OMP performance with $T = 80$ after 50 frames. In Fig. 1(b), we consider time varying channels with $\rho = 0.9$ and set $T = 40$ for the proposed technique, OMP, and AdaOMP. As shown, our technique remains capable to converge at an acceptable NMSE level after 50 frames. However, OMP that does not exploit time correlation, and AdaOMP that ignores the low rank of the received training signals, result in poor performance.

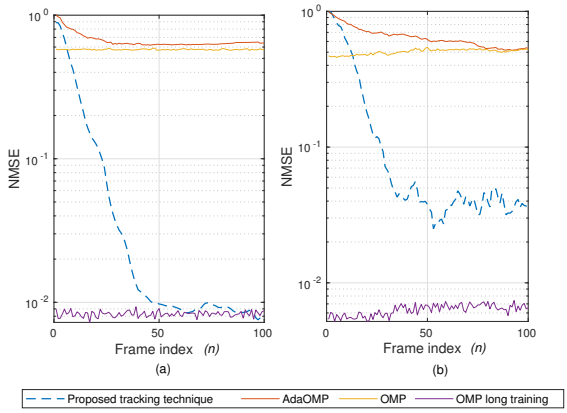

Fig. 1. NMSE performance vs the number of frames with $\sigma_n^2 = 0.3162$ for $\rho = 1$ in (a) and $\rho = 0.9$ in (b).

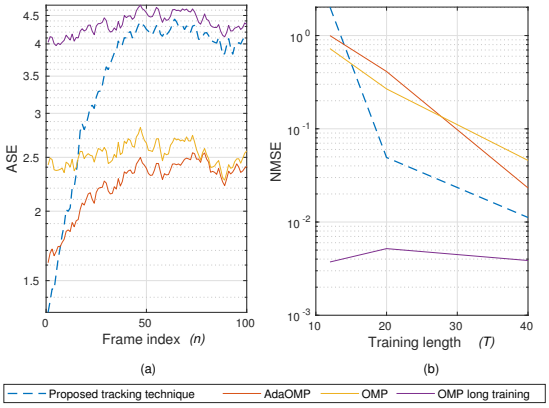

Fig. 2. Performance results with $\rho = 0.9$ and $\sigma_n^2 = 0.3162$ for (a) ASE vs the number of frames and (b) NMSE vs the training length T.

In Fig. 2(a), we plot the Achievable Spectral Efficiency (ASE) for the considered techniques, defined as: ASE $\triangleq \log_2 |\mathbf{I}_{N_{\text{R}}} + \frac{1}{N_{\text{T}} N_{\text{R}}} \frac{1}{\sigma_n^2 + \text{NMSE}} \bar{\mathbf{Z}}_n \bar{\mathbf{Z}}_n|$, considering time varying channels with $\rho = 0.9$. It is depicted that after 50 frames, there is only 7% loss in ASE between the proposed technique with $T = 20$ and the non-adaptive OMP case with $T = 80$. Finally, in Fig. 2(b), the NMSE is illustrated as a function of T, and it is shown to improve with increasing T for all techniques, converging to the performance of OMP with $T = 80$.

5. REFERENCES

[1] T. S. Rappaport, S. Sun, R. Mayzus, H. Zhao, Y. Azar, K. Wang, G. Wong, J. K. Schulz, M. Samim, and F. Gutierrez, "Millimeter wave mobile communications for 5G cellular: It will work!," *IEEE Access*, vol. 1, pp. 335–349, May 2013.

[2] A. F. Molisch, V. V. Ratnam, S. Han, Z. Li, S. L. H. Nguyen, L. Li, and K. Haneda, "Hybrid beamforming for massive MIMO: A survey," *IEEE Commun. Mag.*, vol. 55, no. 9, pp. 134–141, Sept. 2017.

[3] 3GPP, "Study on New Radio (NR) Access Technology-Physical Layer Aspects- Release 14," *3GPP*, TR 38.802, 2017.

[4] A Alkhateeb, O El Ayach, G Leus, and R W Heath Jr., "Channel estimation and hybrid precoding for millimeter wave cellular systems," *IEEE J. Sel. Topics Signal Process.*, vol. 8, no. 5, pp. 831–846, Oct. 2014.

[5] R. Méndez-Rial, C. Rusu, N. González-Prelcic, A. Alkhateeb, and R. W Heath, Jr., "Hybrid MIMO architectures for millimeter wave communications: Phase shifters or switches?," *IEEE Access*, vol. 4, pp. 247–267, Jan. 2016.

[6] J Lee, G T Gil, and Y H Lee, "Channel estimation via orthogonal matching pursuit for hybrid MIMO systems in millimeter wave communications," *IEEE Trans. Commun.*, vol. 64, no. 6, pp. 2370–2386, June 2016.

[7] K. Venugopal, A. Alkhateeb, N. González-Prelcic, and R. W. Heath, Jr., "Channel estimation for hybrid architecture-based wideband millimeter wave systems," *IEEE J. Sel. Areas Commun.*, vol. 35, no. 9, pp. 1996–2009, Sept. 2017.

[8] D. L. Donoho, "Compressed sensing," *IEEE Trans. Inf. Theory*, vol. 52, no. 4, pp. 1289–1306, Apr. 2006.

[9] T. T. Cai and L. Wang, "Orthogonal matching pursuit for sparse signal recovery with noise," *IEEE Trans. Inf. Theory*, vol. 57, no. 7, pp. 4680–4688, July 2011.

[10] D. Lee, S.-J. Kim, and G. B. Giannakis, "Channel gain cartography for cognitive radios leveraging low rank and sparsity," *IEEE Trans. Wireless Commun.*, vol. 16, no. 9, pp. 5953–5966, Sept. 2017.

[11] X. Li, J. Fang, H. Li, and P. Wang, "Millimeter wave channel estimation via exploiting joint sparse and low-rank structures," *IEEE Trans. Wireless Commun.*, vol. 17, no. 2, pp. 1123–1133, Feb. 2018.

[12] E. Vlachos, G. C. Alexandropoulos, and J. Thompson, "Massive MIMO channel estimation for millimeter wave systems via matrix completion," *IEEE Signal Process. Lett.*, vol. 25, no. 11, pp. 1675–1679, Nov. 2018.

[13] E. Vlachos, G. C. Alexandropoulos, and J. Thompson, "Wideband MIMO channel estimation for hybrid beamforming millimeter wave systems via random spatial sampling," *IEEE J. Sel. Topics Signal Process.*, vol. 13, no. 5, pp. 1136–1150, Sept. 2019.

[14] G. C. Alexandropoulos and S. Chouvardas, "Low complexity channel estimation for millimeter wave systems with hybrid A/D antenna processing," in *Proc. IEEE GLOBECOM*, Washington D.C., USA, Dec. 2016, pp. 1–6.

[15] J. He, T. Kim, H. Ghauch, K. Liu, and G. Wang, "Millimeter wave MIMO channel tracking systems," in *Proc. IEEE GLOBECOM*, Austin, USA, 8-12 Dec. 2014, pp. 1–6.

[16] A M Sayeed, "Deconstructing multiantenna fading channels," *IEEE Trans. Signal Process.*, vol. 50, no. 10, pp. 2563–2579, Oct. 2002.

[17] J. F. Cai, E J Candès, and Z Shen, "A singular value thresholding algorithm for matrix completion," *SIAM J. Opt.*, vol. 20, no. 4, pp. 1956–1982, 2010.